An essential role for Fgfs in endodermal pouch formation influences later craniofacial skeletal patterning

Justin Gage Crump[1,*], Lisa Maves[1], Nathan D. Lawson[2], Brant M. Weinstein[3] and Charles B. Kimmel[1]

[1]Institute of Neuroscience, 1254 University of Oregon, Eugene, OR 97403-1254, USA
[2]Program in Gene Function and Expression, University of Massachusetts Medical School, Worcester, MA 01605, USA
[3]Laboratory of Molecular Genetics, NICHD/NIH, Bethesda, MD 20892, USA
*Author for correspondence (e-mail: gage@uoneuro.uoregon.edu)

Accepted 18 August 2004

Development 131, 5703-5716
Published by The Company of Biologists 2004
doi:10.1242/dev.01444

Summary

Fibroblast growth factor (Fgf) proteins are important regulators of pharyngeal arch development. Analyses of Fgf8 function in chick and mouse and Fgf3 function in zebrafish have demonstrated a role for Fgfs in the differentiation and survival of postmigratory neural crest cells (NCC) that give rise to the pharyngeal skeleton. Here we describe, in zebrafish, an earlier, essential function for Fgf8 and Fgf3 in regulating the segmentation of the pharyngeal endoderm into pouches. Using time-lapse microscopy, we show that pharyngeal pouches form by the directed lateral migration of discrete clusters of endodermal cells. In animals doubly reduced for Fgf8 and Fgf3, the migration of pharyngeal endodermal cells is disorganized and pouches fail to form. Transplantation and pharmacological experiments show that Fgf8 and Fgf3 are required in the neural keel and cranial mesoderm during early somite stages to promote first pouch formation. In addition, we show that animals doubly reduced for Fgf8 and Fgf3 have severe reductions in hyoid cartilages and the more posterior branchial cartilages. By examining early pouch and later cartilage phenotypes in individual animals hypomorphic for Fgf function, we find that alterations in pouch structure correlate with later cartilage defects. We present a model in which Fgf signaling in the mesoderm and segmented hindbrain organizes the segmentation of the pharyngeal endoderm into pouches. Moreover, we argue that the Fgf-dependent morphogenesis of the pharyngeal endoderm into pouches is critical for the later patterning of pharyngeal cartilages.

Key words: Pouch, Pharyngeal endoderm, Cartilage, Neural crest, Segmentation, Fgf8, Fgf3, *acerebellar*, GFP, Zebrafish

Introduction

The cartilages and bones that form the skeleton of the face and, in mammals, the middle ear, are derived from a specialized population of ectomesenchyme, the cranial neural crest (Le Douarin, 1982; Weston et al., 2004). Cranial neural crest cells (NCC) originate adjacent to neural ectoderm and migrate in three streams (mandibular, hyoid and branchial) to form seven pharyngeal arches. Segmentation of NCC into distinct streams is coupled to the segmentation of the hindbrain into rhombomeres (R1-7) (Kontges and Lumsden, 1996). NCC that contribute to the formation of the mandibular arch delaminate adjacent to posterior midbrain-R2 and do not express Hox genes, whereas NCC of the hyoid and branchial arches originate next to R4 and R6-R7, respectively, and are Hox-positive (Schilling and Kimmel, 1994; Trainor and Krumlauf, 2001).

Fibroblast growth factors (Fgfs) are a family of extracellular signaling molecules that have been implicated in diverse facets of vertebrate craniofacial development. Fgf8 from the oral surface ectoderm induces patterns of gene expression in adjacent mandibular mesenchyme, subdividing the mandibular arch into rostral odontogenic and caudal skeletogenic fields (Tucker et al., 1999) and controlling the position of the jaw joint (Wilson and Tucker, 2004). In addition to functions in mandibular arch development, Fgfs have roles in the development of cartilages derived from the hyoid and branchial arches and in the formation of pharyngeal pouches. Pouches are outpocketings of the pharyngeal endoderm that interdigitate with the crest-derived pharyngeal arches. *Fgf8*$^{neo/-}$ mice, which are hypomorphic for *Fgf8*, display a range of craniofacial abnormalities that include reductions in cartilages and bones derived from all pharyngeal arches and disorganized endodermal pouches (Abu-Issa et al., 2002). Likewise, in the zebrafish *acerebellar* (*ace*) mutant, a strong loss-of-function mutation of *fgf8* (hereafter referred to as *fgf8*$^{-}$), hyoid cartilage is reduced and pouches are misshaped (Draper et al., 2001; Reifers et al., 1998; Roehl and Nusslein-Volhard, 2001).

Increasing evidence suggests that signals from the pharyngeal endoderm pattern the bones and cartilages of the pharyngeal arches. Analysis of *casanova* (*cas*) mutant zebrafish, which make no endoderm (Alexander et al., 1999), suggest that endoderm is required for the development of all pharyngeal cartilages (David et al., 2002). In *tbx1* (*van gogh*) mutant zebrafish, pharyngeal pouches are largely absent and cartilages are misshaped and fused with those of adjacent arches (Piotrowski and Nusslein-Volhard, 2000), suggesting that pouches contribute to the segmentation of NCC into distinct arches. In addition, transplantation experiments in chick show that foregut endoderm is both necessary and sufficient to induce the shape and orientation of pharyngeal skeletal elements (Couly

et al., 2002). One role of pharyngeal endoderm may be to locally promote the survival of skeletogenic NCC (Crump et al., 2004). Fgf3 has been shown to be required in pouch endoderm for the survival of skeletogenic NCC of the hyoid and branchial arches (David et al., 2002; Nissen et al., 2003), and a similar NCC survival-promoting role for endodermal Fgf8 has been proposed but not proven in zebrafish (Walshe and Mason, 2003a). Clearly, understanding how pharyngeal endoderm develops is critical for understanding the later development of the pharyngeal skeleton.

In this study, we investigate an earlier role for Fgfs in the formation of pharyngeal pouches. Whereas in *fgf8*$^{-}$ animals pharyngeal pouches are variably misshaped, we find that reducing both Fgf8 and Fgf3, by injecting *fgf8*$^{-}$ animals with an *fgf3* morpholino (*fgf3*-MO), leads to a complete failure of pouch formation. We use time-lapse microscopy to show that pharyngeal pouches form by the directed lateral migration of periodic clusters of endodermal cells. In *fgf8*$^{-}$; *fgf3*-MO animals, pharyngeal endodermal cells are present but their lateral migration is disorganized and discrete pouches fail to form. We use the Fgf receptor-inhibiting drug SU5402 to show that Fgf signaling is required during early somite stages for first pouch formation. At these stages, *fgf8* is expressed in the head in lateral mesoderm (Reifers et al., 2000) and in midbrain-hindbrain boundary (MHB)-R2 and R4 domains of the hindbrain (Maves et al., 2002; Reifers et al., 1998). Starting at 4-somites (11.3 hours post-fertilization), *fgf3* expression overlaps *fgf8* expression in neural MHB and R4 domains (Maves et al., 2002; Walshe et al., 2002), and mesodermal and neural Fgf expression domains are in close proximity to developing pharyngeal endoderm. At later stages, *fgf3* and, to a lesser extent, *fgf8* are expressed in the pharyngeal pouches (David et al., 2002; Walshe and Mason, 2003a). However, we use mosaic analysis to show that Fgfs are required in mesodermal and neural domains, and not in the pharyngeal endoderm, to rescue pharyngeal arch structure in *fgf8*$^{-}$; *fgf3*-MO animals. Thus, we find an essential, Fgf-dependent function of the brain and head mesoderm in controlling segmentation of the pharyngeal endoderm into pouches.

In addition to their requirement in pouch formation, we find that Fgf8 and Fgf3 have redundant, essential functions in pharyngeal cartilage development. In *fgf8*$^{-}$; *fgf3*-MO animals, hyoid and branchial cartilages are largely absent and mandibular cartilages are reduced. By imaging pouch structure early and cartilage structure later in individual sides of animals in which Fgf signaling has been manipulated, we find that altered pouches correlate with later rearrangements of the cartilage pattern. This analysis suggests that pharyngeal pouch structure is a critical determinant of the pharyngeal cartilage pattern. We present a model in which an earlier function of Fgfs in pouch formation, in addition to their well-documented role as pouch-secreted survival factors later in development, contributes to the diversity of craniofacial phenotypes seen in *fgf8* mutants.

Materials and methods

Zebrafish lines and morpholinos

Zebrafish (*Danio rerio*) were raised and staged as previously described (Kimmel et al., 1995; Westerfield, 1995). Time (hpf) refers to hours post-fertilization at 28.5°C. The wild-type line used was AB. Homozygous *acerebellar*^{ti282a} (*ace*) mutant embryos were scored by their loss of the cerebellum or loss of midbrain *pax2a* expression (Brand et al., 1996; Reifers et al., 1998). *fli1*-GFP albino transgenic fish are the same as *TG(fli1:EGFP)*^{y1}*; alb*^{b4} (Lawson and Weinstein, 2002) and H2A.F/Z:GFP transgenic fish are as described (Pauls et al., 2001).

The *fgf8* MOs E2I2 and E3I3 (Draper et al., 2001) were used at 0.5 mg/ml each. To generate *fgf8*$^{-}$; *fgf3*-MO embryos, we pressure-injected *fgf8*$^{-}$ embryos at the one-cell stage with 5 nl of the *fgf3*B (1.0 mg/ml) + *fgf3*C (0.25 mg/ml) MO combination. As previously described (Maves et al., 2002), this *fgf3* MO dose gave highly reproducible *fgf8*$^{-}$; *fgf3*-MO phenotypes, scored as either the lack of ears or the lack of R5 *krox20* staining.

Phenotypic analysis

Alcian Green staining was performed as described (Miller et al., 2003). For flat-mount dissections, Alcian-stained animals were digested for 1 hour in 8% trypsin at 37°C and transferred to 100% glycerol. Cartilages were dissected free from surrounding tissues with fine stainless-steel insect pins and photographed using a Zeiss Axiophot 2 microscope. Image background was cleaned up with Adobe Photoshop. For immunocytochemistry, embryos were prepared as described (Maves et al., 2002). Antibodies were used at the following dilutions: rabbit anti-GFP, 1:1000 (Molecular Probes); Zn8, 1:400 (Fashena and Westerfield, 1999; Trevarrow et al., 1990), goat anti-rabbit Alexa Fluor 488 and anti-mouse Alexa Fluor 568, both 1:300 (Molecular Probes).

The following cDNA probes were used: *dlx2* (Akimenko et al., 1994); *krox20* (Oxtoby and Jowett, 1993); *pax2a* (Krauss et al., 1991); *axial* (Odenthal and Nusslein-Volhard, 1998); *nkx2.7* (Lee et al., 1996); *pea3* (Brown et al., 1998). Probe syntheses and whole-mount in-situ hybridizations were performed as previously described (Hauptmann and Gerster, 1994; Jowett and Lettice, 1994).

SU5402 treatment

fli1-GFP embryos were manually dechorionated and incubated in 40 μl of EM with 0.4 mM SU5402 (Calbiochem) in agar wells. SU5402 was diluted from a 40 mM stock in DMSO. After 1- or 4-hour incubations, embryos were washed vigorously in EM. For 4-hour incubation experiments, sibling controls were fixed and processed for in-situ hybridizations with *pea3*.

Transplantations

Transplant techniques were as described (Maves et al., 2002). For endoderm transplants, donor embryos were injected at the 1-cell stage with an 'Alexa568' mixture of 2% Alexa Fluor 568 dextran and 3% lysine-fixable biotin dextran (10,000 M_r, Molecular Probes) along with activated Taram-A receptor (TAR*) RNA prepared according to David et al. (David et al., 2002). At 40% epiboly (ca. 4 hpf) donor TAR* tissue was moved to the margins of *fgf8*$^{-}$; *fgf3*-MO; *fli1*-GFP host embryos. For neural and mesodermal transplants, donor embryos were injected at the 1-cell stage with Alexa568. For neural transplants, donor tissue was taken from the animal cap at shield stage (ca. 6 hpf) and moved to a position approximately two germ ring widths from the margin and 70° from dorsal in *fgf8*$^{-}$; *fgf3*-MO; *fli1*-GFP hosts (Maves et al., 2002). For mesodermal transplants, donor tissue was taken from the margin at 50% epiboly (ca. 5 hpf) and moved to the margins of *fgf8*$^{-}$; *fgf3*-MO; *fli1*-GFP hosts (Kimmel et al., 1990). All hosts were screened using a fluorescence stereomicroscope at 34 hpf, and only hosts with substantial, tissue-specific contributions to the pharyngeal endoderm, hindbrain or cranial mesoderm were used for subsequent analysis. In addition, the mesodermal transplant technique produced six embryos with contributions to both the hindbrain and cranial mesoderm. In order to control for variability in the effectiveness of the *fgf3*-MO, only *fgf8*$^{-}$; *fgf3*-MO; *fli1*-GFP hosts in which the ear was missing in at least one side were used for the analysis. In control transplants, mutant siblings in which donor tissue did not contribute to head tissues, we never observed the presence of an ear on only one side. At 34 hpf, confocal images of select host embryos were analyzed for pharyngeal arch structure. Rescue of arch structure was scored as complete if the first pouch and mandibular and hyoid arches were indistinguishable from

wild type, and rescue was scored as partial for all other embryos with arch structure subjectively more organized than in *fgf8*⁻; *fgf3*-MO; *fli1*-GFP controls.

Time-lapse analysis and confocal imaging

For the endoderm movies (see Movies 3-6 in supplementary material), pharyngeal endoderm was labeled by transplanting donor tissue injected with a mixture of Alexa568 and TAR* into GFP hosts. Embryos were selected for large fractions of labeled donor endoderm and bright GFP fluorescence using a Leica MZ FLIII fluorescence stereomicroscope. After manual dechorionation and anesthetization with buffered ethyl-*m*-aminobenzoate methane sulfanate (MESAB) (Westerfield, 1995), embryos were transferred to 0.2% agarose in embryo media (EM) with 10 mM HEPES and MESAB and then mounted onto a drop of 3% methylcellulose on a rectangular coverslip with three superglued #1 square coverslips on each side. A ring of vacuum grease was added around the embryo to make an airtight seal upon addition of the top coverslip. A heated stage kept the embryos at 28.5°C. Approximately 80 μm Z-stacks at 2 μm intervals were captured every 6 minutes using a Zeiss LSM5 Pascal confocal fluorescence microscope. At each time point, Z-stacks were projected with maximum intensity onto a single plane. Time-lapse recordings were further processed with Adobe Premiere. For single time point confocal sections, embryos were mounted without vacuum grease.

Results

Fgf8 and Fgf3 are essential for the formation of pharyngeal pouches and most pharyngeal cartilages

As previously reported (Roehl and Nusslein-Volhard, 2001), *fgf8*⁻ zebrafish had incompletely penetrant and expressive defects in the formation of pharyngeal pouches and cartilages (Fig. 1B,B′,F and especially Fig. 2I,J). Since the *fgf8*⁻ phenotype is relatively mild, we wondered if other Fgfs were partially redundant with Fgf8 in patterning pharyngeal arches. Fgf3 was a good candidate, as it has been shown to act redundantly with Fgf8 to pattern the posterior hindbrain, forebrain and ear (Maroon et al., 2002; Maves et al., 2002; Phillips et al., 2001; Walshe et al., 2002; Walshe and Mason, 2003b). In addition, Fgf3 has been shown to play a role in zebrafish pharyngeal arch development (David et al., 2002; Nissen et al., 2003). Although *fgf3*-MO animals had largely normal pouches (Fig. 1C,C′) (David et al., 2002), we found that in *fgf8*⁻; *fgf3*-MO animals no pouches were made (Fig. 1D,D′). In addition, we found that Fgf8 and Fgf3 acted redundantly to promote pharyngeal cartilage development. In *fgf3*-MO animals, the ceratobranchial (CB) cartilages, which derive from the branchial arches located posterior to the hyoid arch, were largely absent (David et al., 2002; Nissen et al., 2003). However, whereas hyoid cartilages of *fgf3*-MO and *fgf8*⁻ animals were relatively mildly affected at 4 days (Fig. 1F,G), nearly all of the hyoid and CB cartilages in *fgf8*⁻; *fgf3*-MO animals were absent (Fig. 1H). Although reduced in size, mandibular cartilages were patterned correctly in *fgf8*⁻; *fgf3*-MO animals (inset to Fig. 1H).

Since *fgf8*⁻; *fgf3*-MO animals have both pouch and cartilage defects, we wondered whether defects in pouch development could be responsible for later cartilage losses. In order to study correlations between pouch and cartilage defects in individual animals, we took advantage of the fact that partially reducing

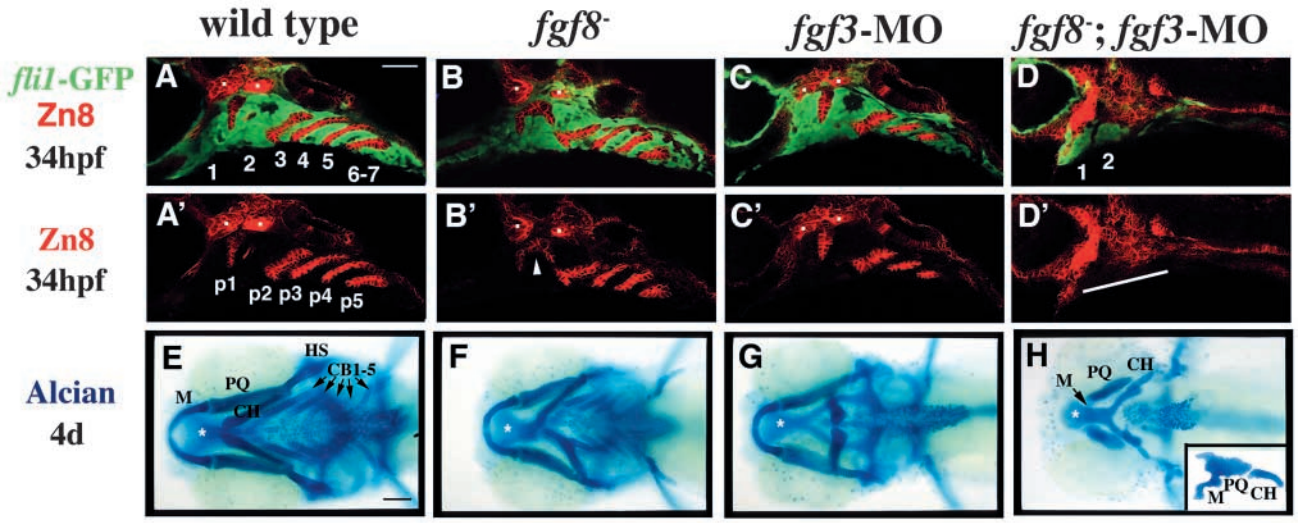

Fig. 1. Fgf8 and Fgf3 have redundant functions in the formation of pharyngeal pouches and cartilages. (A-D) Confocal micrographs are merged, lateral views of cranial NCC (green: anti-GFP antibody) and endodermal pouches (red: Zn8 antibody) at 34 hpf; A′-D′ show just the red channel. (A,A′) In wild-type *fli1*-GFP animals, the NCC-containing pharyngeal arches are numbered 1-7 (A) and the pouches are numbered p1-p5 (A′). A few hours later, the sixth pouch will form and arches 6 and 7 will separate to form the final arrangement of seven arches. (B,B′) *fgf8*⁻*; fli1*-GFP animals have variable defects in pouch structure (arrowhead in B′ denotes a misshapen first pouch). Whereas *fgf3*-MO; *fli1*-GFP animals have normal pouches (C,C′), *fgf8*⁻; *fgf3*-MO; *fli1*-GFP animals lack all pouches (D,D′), although pharyngeal endoderm is still present (white line in D′). The Zn8 antibody also recognizes cranial sensory ganglia (dots in A-C, A′-C′). (E-H) Ventral whole-mount views show Alcian-stained pharyngeal cartilages at 4 days. As shown for wild type (E), M and PQ cartilages are derived from the mandibular, or first, arch; CH and HS are hyoid, or second, arch cartilages, and CB1-5 cartilages are formed from the five most posterior branchial arches. *fgf8*⁻ animals have relatively mild defects in pharyngeal cartilages (F), and in *fgf3*-MO animals CB cartilages are lost and hyoid cartilages are misshapen (G). However, in *fgf8*⁻; *fgf3*-MO animals, nearly all CB and hyoid cartilages are absent and mandibular cartilages are reduced in size (H). The inset to H is a flat-mount preparation of *fgf8*⁻; *fgf3*-MO cartilages showing that, although reduced in size, M and PQ cartilages retain their distinctive shapes. In E-H, asterisks denote the position of the midline neurocranium that is still present in *fgf8*⁻; *fgf3*-MO animals. Anterior is to the left in all panels. M, Meckel's; PQ, palatoquadrate; CH, ceratohyal; HS, hyosymplectic; CB, ceratobranchial. Scale bars: 50 μm in A-D; 100 μm in E-H.

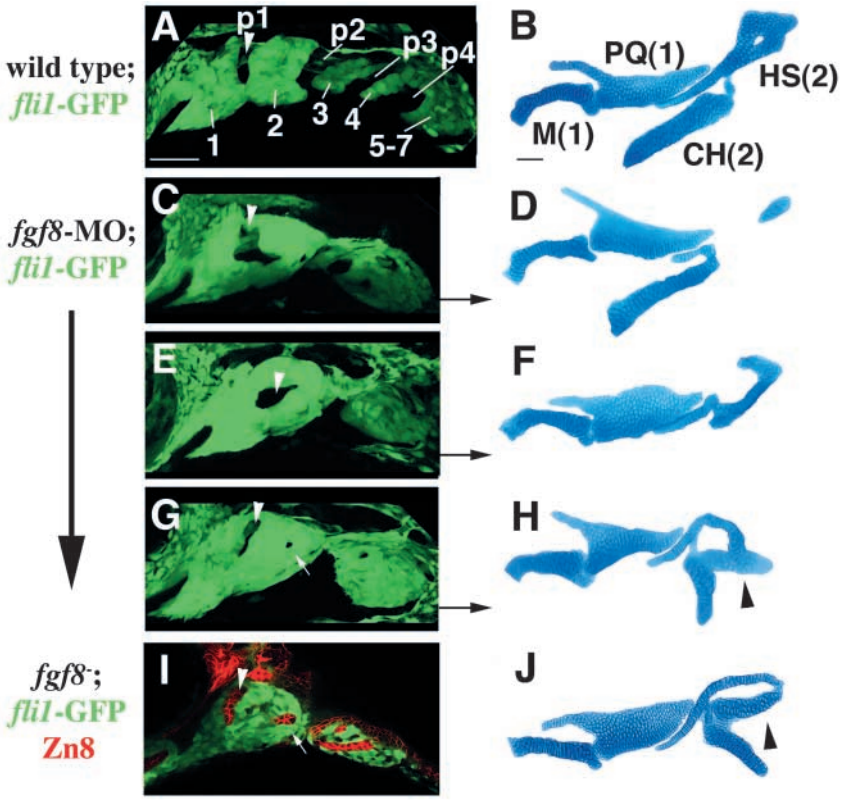

Fig. 2. Correlated first pouch and hyoid cartilage defects in animals reduced for Fgf8. Confocal projections of *fli1*-GFP-labeled pharyngeal arches in living wild-type (A) and *fgf8*-MO (C,E,G) animals at 28 hpf. By this stage of wild-type development, the mandibular (1), hyoid (2), and three branchial arches (3, 4, 5-7) have formed. Pouches are labeled p1-p4 (A), and white arrowheads mark the positions of the first pouch. In *fgf8*-MO; *fli1*-GFP animals, variable phenotypes include shape changes in the first pouch (C,E), ectopic pouches (arrow in G), and reductions of more posterior pouches (C,E,G). (I) Confocal micrograph of a fixed *fgf8*$^{-}$; *fli1*-GFP animal with a similar ectopic pouch phenotype (arrow) to the *fgf8*-MO; *fli1*-GFP animal in G; Zn8 staining (red) confirms that the non-*fli1*-GFP-expressing region is probably an ectopic endodermal pouch. (B,D,F,H,J) Flat-mount preparations of Alcian-stained mandibular and hyoid cartilages at 4 days. As labeled in the wild-type example (B), M and PQ are mandibular (1) and CH and HS are hyoid (2) cartilages. (C and D, E and F, G and H) Paired images of individual animals imaged live for *fli1*-GFP early and subsequently stained for cartilage. Variable hyoid cartilage defects (D,F,H) are correlated with earlier first pouch defects (C,E,G) in individual *fgf8*-MO; *fli1*-GFP animals. In H, the black arrowhead marks an apparent ectopic hyoid cartilage that correlates with the ectopic pouch in G. (J) Similar ectopic cartilages (black arrowhead) were seen in some *fgf8*$^{-}$; *fli1*-GFP animals. Anterior is to the left and dorsal is up. M, Meckel's; PQ, palatoquadrate; CH, ceratohyal; HS, hyosymplectic. Scale bar: 50 μm.

Fgf function with an *fgf8* morpholino (*fgf8*-MO), or genetically with the *fgf8* mutation, causes variably penetrant and expressive phenotypes. We imaged pharyngeal arch structure in live *fgf8*-MO; *fli1*-GFP and *fgf8*$^{-}$; *fli1*-GFP embryos at 28 hpf and subsequently raised individuals to 4 days to examine cartilage. The *fli1*-GFP transgene (Lawson and Weinstein, 2002) labels cranial NCC shortly after ventrolateral migration and perdures as cells differentiate into the pharyngeal cartilage elements. *fli1*-GFP also marks the developing vasculature but is not expressed in the pharyngeal mesoderm or endoderm (except for early, transient expression in the second pouch; see below). At pharyngula stages, the endodermal pouches are evident as non-*fli1*-GFP-expressing regions separating the *fli1*-GFP-expressing NCC of the pharyngeal arches (black in Fig. 2A). In individual sides of *fgf8*-MO; *fli1*-GFP and *fgf8*$^{-}$; *fli1*-GFP animals we found a correlation between early arch structure and alterations of the hyoid cartilage pattern (Fig. 2C-J and Table 1). In all sides with abnormal first pouch morphology we observed hyoid cartilage alterations later. In some cases, the first pouch was 'deformed' (Fig. 2C), invading hyoid NCC territory, and this arch phenotype was most often linked to a complete loss of the dorsal hyomandibular cartilage element (Fig. 2D). In other cases, the first pouch was 'shifted' to a more posterior position (Fig. 2E), and this 'shift' was correlated with changes in the shape and position of dorsal hyoid cartilage (Fig. 2F). In the most striking example of pouch–cartilage shape correlations, a small ectopic pouch, in addition to the normal first pouch, formed in the middle of the hyoid NCC territory (Fig. 2G), and in these same sides an ectopic cartilage element developed later in the hyoid arch (Fig. 2H). To confirm that the non-GFP-expressing regions observed in live animals probably corresponded to misshapen and ectopic pouches, and not another non-GFP-expressing tissue such as mesoderm, we fixed and stained *fgf8*$^{-}$ animals displaying similar GFP phenotypes with the endoderm-labeling Zn8 antibody (Trevarrow et al., 1990). In numerous examples, non-GFP expressing regions in *fgf8*$^{-}$ animals, of similar shapes and positions to those observed in the live analysis, were found to be Zn8-positive (red in Fig. 1B and Fig. 2I; and data not shown). Lastly, whereas the majority of *fgf8*$^{-}$ animals with normal arch morphology early had no defects in the hyoid cartilage pattern later, we observed graded reductions of the hyomandibular cartilage element in some sides with no pouch defects (Table 1). Thus, Fgf8 is likely to have other functions in cartilage development, in addition to its role in controlling pouch development. Nonetheless, we conclude that, in contrast to simple cartilage losses, the alterations in hyoid cartilage shape and position observed in a subset of animals reduced for Fgf8 are most tightly correlated with early changes in pouch morphology.

Posterior pharyngeal pouch defects underlie reduced arch segmentation in *fgf8*-MO animals

After NCC migration the third, most posterior, NCC mass segments into the five branchial, or gill-bearing, arches from which the five CB cartilages subsequently develop (Fig. 3A). It has been previously shown that the segmentation of NCC into distinct arches requires the segmentation of the pharyngeal

Table 1. Correlated pouch and cartilage phenotypes in *fgf8*⁻; *fli1*-GFP animals

		Hyoid cartilage phenotype					
Arch structure	%(*n*)	Wild type	HM reduced	HM loss	Ventral loss	Shape change	Ectopic
Wild type	74	**59**	33	2	0	6	0
No p1	2	0	**100**	0	0	0	0
Deformed p1	6	0	0	**88**	0	12	0
Shifted p1	2	0	0	0	0	**100**	0
Ectopic p1	5	0	0	0	0	**50**	**50**
Arch shape	12	7	13	13	20	**40**	7

Percentage of sides with each phenotype is listed for *fgf8*⁻; *fli1*-GFP animals (*n*=128). In 100 wild-type animals, none of these phenotypes were seen. At 33 hpf, individual sides of *fgf8*⁻; *fli1*-GFP mutant animals were scored under a fluorescence dissecting microscope for pharyngeal arch structure. Hyoid arches of mutant sides were scored as percentage of the total having the following morphology: wild type, missing the first pouch (no p1), deformed first pouch (deformed p1), shifted first pouch (shifted p1), ectopic first pouch in addition to normal first pouch (ectopic p1), and miscellaneous defects that affected arch shape but not first pouch structure (arch shape). Individuals were subsequently grown to 4 days to examine hyoid cartilage structure. Percentages of each arch structure category having the following hyoid cartilage phenotypes are shown: wild type, reduction of HM (HM reduced), loss of HM (HM loss), loss of ventral cartilage (ventral loss), rearrangement of the cartilage pattern (shape change), and ectopic cartilage elements (ectopic).

endoderm into pouches (Piotrowski and Nusslein-Volhard, 2000). In animals reduced for Fgf8, we observed a range of CB cartilage phenotypes that suggests defects in the segmentation of NCC into distinct branchial arches. These phenotypes include reductions in the number of CB cartilages (Fig. 3B) and fusions of cartilages of adjacent segments (Fig. 3C); incompletely formed CB cartilages were also observed (Fig. 3C). In addition, as reported for *fgf8*⁻ animals (Roehl and Nusslein-Volhard, 2001), more posterior pharyngeal pouches were reduced and disorganized in *fgf8*-MO; *fli1*-GFP animals (Fig. 2C,E,G). We investigated whether the CB cartilage defects seen in *fgf8*-MO animals might be secondary to posterior pouch formation defects that result in reduced branchial NCC segmentation.

In order to understand the cellular basis of NCC segmentation, we made time-lapse recordings of pharyngeal arch development in wild-type (see Movie 1 in supplementary material) and *fgf8*-MO (see Movie 2 in supplementary material) animals. Time-lapse recordings were made of wild-type animals expressing both the pan-nuclear H2A.F/Z:GFP and the NCC-expressing *fli1*-GFP (12-38 hpf; Movie 1). In wild-type animals, NCC migrated in three streams to ventrolateral regions, where they contributed to the formation of the pharyngeal arches. Starting at 12 hpf (5-somites), H2A.F/Z:GFP-labeled NCC were seen migrating in two streams (mandibular and hyoid) anterior to, and one stream (branchial) posterior to, the developing otic vesicle. By around 16 hpf, the NCC finished their migration and began to express *fli1*-GFP as they condensed to form the arch masses. Shortly after the initiation of *fli1*-GFP expression in NCC, the first branching of the branchial mass occurred as the third pouch was formed (Fig. 3D). Over the next 20 hours, the fourth, fifth and sixth pouches formed in an anterior-posterior (AP) wave of development, and by 38 hpf the branchial mass had been subdivided into the five segments from which the CB cartilages would arise (Fig. 3E-G).

By contrast, in the *fgf8*-MO; *fli1*-GFP example shown (see Movie 2 in supplementary material), one fewer branchial segment formed. We found that in this animal the reduced number of segments was due to the failure of the fourth pouch to develop. While the third pouch (i.e. the first pouch to subdivide the branchial mass) formed normally (Fig. 3H), the fourth pouch initiated outgrowth yet failed to fully subdivide the branchial mass into a new segment (Fig. 3I). By 38 hpf the fifth and sixth pouches had fully formed, but the fourth pouch had retracted, and what in wild-type animals would have been the second and third posterior branchial segments had fused together, resulting in one less branchial segment (Fig. 3J,K). Consistent with this animal forming one less branchial segment, we found that one less CB cartilage developed (data not shown). These results suggest that at least some, and possibly all, of the CB cartilage defects seen in *fgf8*⁻ animals are the result of a failure of posterior endodermal pouches to form properly and segment branchial NCC into discrete arches.

Fgf signaling is required during early somite stages for first pouch development

In order to determine when Fgfs act to control pouch development, we inhibited Fgf signaling at different times of development using the Fgf receptor antagonist SU5402. As extended (24-hour) treatment of embryos with SU5402 causes widespread death of NCC (David et al., 2002), we performed shorter treatments of SU5402 in order to dissociate requirements for Fgf signaling in pharyngeal pouch formation from those in NCC survival. After addition of SU5402 for 1- to 4-hour periods, followed by a washout, embryos were scored for pouch defects at 34 hpf. In the case of 4-hour treatments, we examined effectiveness of inhibition of Fgf signaling by expression of the Ets factor, *pea3*, in treated siblings. *pea3* is a downstream target of Fgf signaling (Roehl and Nusslein-Volhard, 2001), and we observed partial-to-complete inhibition of *pea3* expression during the treatment and gradual recovery after washout (data not shown, summarized in Fig. 4 legend). In embryos treated with SU5402 from 10 to 14 hpf, we found that the first pouch was specifically lost in 39% of embryos (Fig. 4B) and misshapen in another 26% of embryos (data not shown). In addition, when animals with first pouch defects were raised to 4 days, we observed specific losses of hyoid cartilage (Fig. 4E). By contrast, SU5402 treatments from 6 to 10 hpf and 14 to 18 hpf had lesser effects on pouch development (Fig. 4G). We found a similar temporal requirement for Fgf signaling using 1-hour SU5402 treatments (Fig. 4C,H). The highest penetrance of first pouch shape defects was seen when 1-hour SU5402 treatments began between 9 and 13 hpf. Interestingly, later (>20 hpf) treatments with SU5402 produced variable

defects in the development of more posterior pouches but not the first pouch (Fig. 4F), consistent with more posterior pouches forming later in an AP temporal wave of development. In summary, we find that Fgf signaling has a peak requirement in first pouch development from 10 hpf (tailbud) to 14 hpf (10-somites).

Neural and mesodermal requirement for Fgfs in pharyngeal pouch formation

As Fgf8 and Fgf3 are expressed in neural and mesodermal tissues at early somite stages, and then in the pharyngeal endoderm at later stages, we investigated which Fgf sources are required for pouch formation. Using transplantation techniques (see Materials and methods), we introduced wild-type tissues at pre-shield stages (<6 hpf) into *fgf8*$^{-}$*; fgf3*-MO; *fli1*-GFP embryos and then assayed for rescue of first pouch development based on GFP-labeled arch structure. First, we found that wild-type endoderm was not able to rescue first pouch structure (Fig. 5B-B″) compared with control contralateral sides that did not receive transplants (Fig. 5A-A″). Wild-type mesoderm (Fig. 5C-C″) or neural tissue (Fig. 5D-D″) alone was able to only partially rescue pouch and arch structure in less than half of *fgf8*$^{-}$*; fgf3*-MO; *fli1*-GFP hosts (Fig. 5F). By contrast, transplantation of wild-type neural and mesodermal tissues together completely rescued pouch structure in 3/6 embryos, and partial rescue was seen in another 2/6 embryos (Fig. 5E-E″). As neural tube transplants alone were sufficient to rescue the ear and cerebellar defects of *fgf8*$^{-}$*; fgf3*-MO embryos (Fig. 5D‴), yet failed to completely rescue pouch structure (Fig. 5D′), we conclude that the requirements for both neural and mesodermal tissues is not simply a function of restoring neural structure in *fgf8*$^{-}$*; fgf3*-MO embryos. Thus,

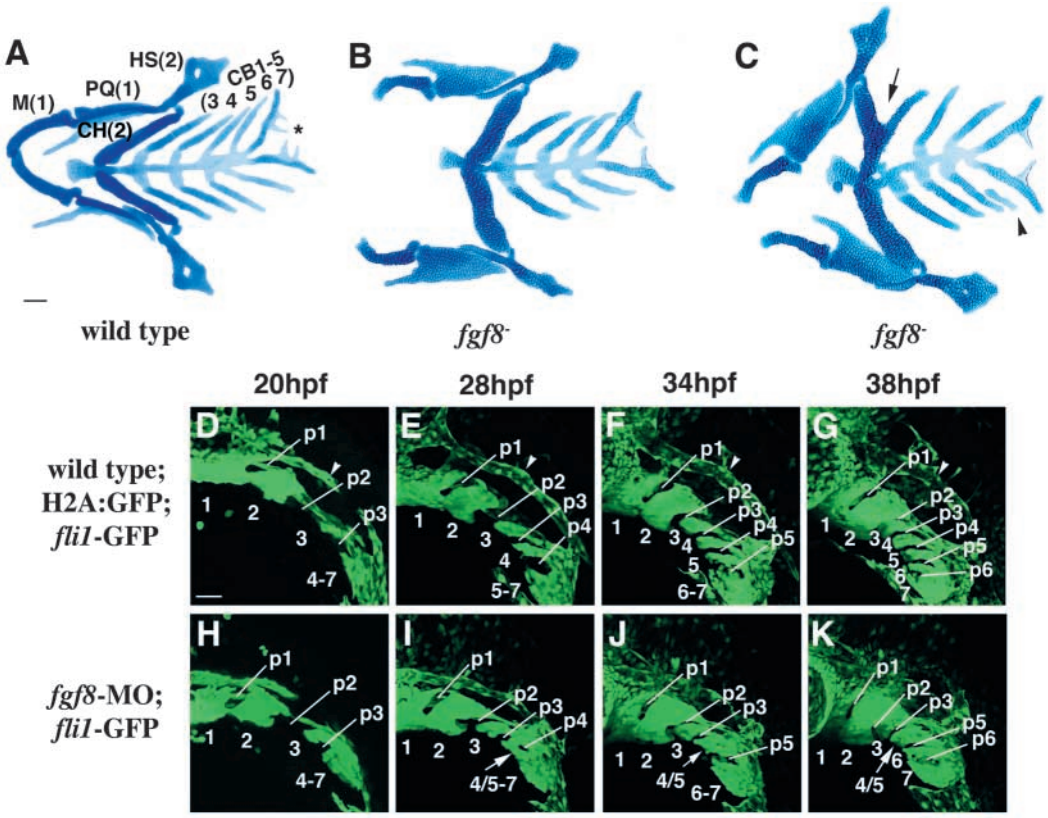

Fig. 3. Fgf8 is required for segmentation of the branchial arches. Bilateral flat-mount dissections of Alcian-stained pharyngeal cartilages at 4 days. As shown for wild type (A), M and PQ are mandibular (1) cartilages, CH and HS are hyoid (2) cartilages, and CB1-5 cartilages are formed from the five most posterior branchial arches (3-7). Note the teeth (*) on the CB5 cartilages. *fgf8*$^{-}$ animals have variable CB cartilage defects, which include reduced CB number (only 4 CBs per side in B), incompletely formed CB cartilages (arrowhead in C), and fusions between adjacent cartilages (arrow in C). In a representative *fgf8*$^{-}$; *fli1*-GFP clutch (n=172) there was an average of 3.9 CB cartilages per side; 6% of sides had fusions of adjacent cartilages and 2% had incomplete cartilages. (D-K) Time-lapse recordings of wild-type *fli1*-GFP; H2A.F/Z:GFP (D-G, and see Movie 1 in supplementary material) and *fgf8*-MO; *fli1*-GFP (H-K, and see Movie 2 in supplementary material) animals show the cellular basis of branchial arch segmentation. In wild-type animals, branchial arches form as pouches separate the branchial NCC mass into segments in an A–P wave of development. At the beginning of Movie 1 (5-somites, 12 hpf), H2A.F/Z:GFP labels the nuclei of NCC that are migrating ventrolaterally in two streams anterior to, and one stream posterior to, the developing ear. After *fli1*-GFP initiates in NCC of the pharyngeal arches, selected projections from Movies 1 and 2 show the subdivision of each successive branchial arch (arch 3 at 20 hpf: D,H; arch 4 at 28 hpf: E,I; arch 5 at 34 hpf: F,J; and arches 6 and 7 at 38 hpf: G,K). Pouches are labeled p1-p6, and white arrowheads in D-G indicate the developing vasculature that also expresses *fli1*-GFP. The white arrows in panels I-K and Movie 2 (in supplementary material) refer to arches 4 and 5, which fail to separate completely in this *fgf8*-MO animal. Similar cell behaviors were seen in three time-lapse recordings of wild-type animals, and variable defects were observed in four time-lapse recordings of *fgf8*-MO; *fli1*-GFP animals. Anterior is to the left in all panels. A-C are ventral views, and dorsal is up and slightly to the right in D-K. M, Meckel's cartilage; PQ, palatoquadrate; CH, ceratohyal; HS, hyosymplectic; CB, ceratobranchial. Scale bar: 50 μm.

Fgf8 and Fgf3 are required additively in both the neural tube and mesoderm, but not the endoderm, to promote morphogenesis of the pharyngeal endoderm into pouches.

Fgf8 and Fgf3 are required for the subsequent development, and not the generation, of pharyngeal endoderm and NCC

In order to test whether the lack of pouches is due to a general reduction in pharyngeal endoderm, we examined early markers of pharyngeal endoderm in *fgf8*$^{-}$; *fgf3*-MO animals. In wild-type embryos, the first pouch began to form around 16 hpf (see below). At 18 hpf, *nkx2.7* and *axial* normally were expressed in lateral pharyngeal endoderm, in particular the first pouch and regions where the second and more posterior pouches would form (Fig. 6A,E). In *fgf3*-MO animals, *nkx2.7* and *axial* expression was similar to that seen in wild-type animals (Fig. 6C,G), whereas in *fgf8*$^{-}$ animals *nkx2.7* and *axial* were present but first pouch staining was variably absent (Fig. 6B,F). Strikingly, in *fgf8*$^{-}$; *fgf3*-MO animals, these markers revealed that a significant amount of pharyngeal endoderm was present, yet there was no clear evidence of pouches (Fig. 6D,H). In addition, as assayed by *axial* staining, we saw no differences in the amount of pharyngeal endoderm at an earlier stage (10 hpf) between *fgf8*$^{-}$; *fgf3*-MO and wild-type animals (data not

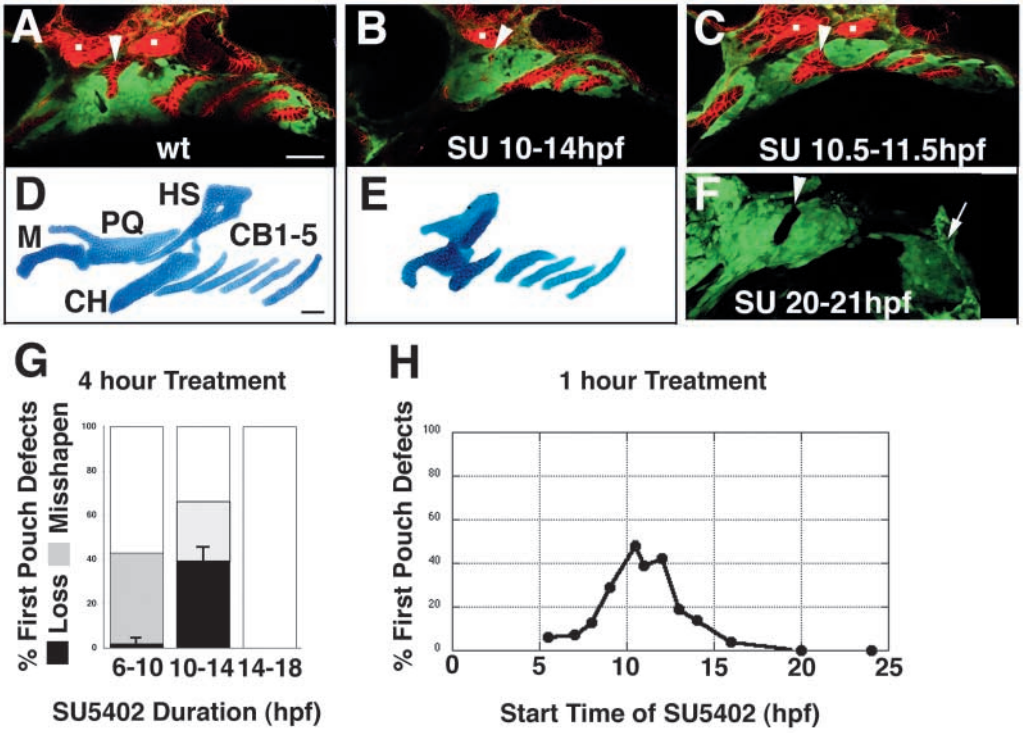

Fig. 4. Fgf signaling is required during early somite stages for first pouch and hyoid cartilage development. (A-C) Confocal micrographs show Zn8-labeled pharyngeal pouches (red) and GFP-labeled NCC (green) in *fli1*-GFP animals at 34 hpf. Cranial sensory ganglia (dots) also stain with Zn8. In the wild-type animal (A), an arrowhead marks the first pouch. (B) The first pouch is variably absent (arrowhead) in *fli1*-GFP animals upon treatment with the Fgf receptor antagonist SU5402 from 10-14 hpf. The absence of the first pouch is selective, as more posterior pouches form normally. (C) Treatment with SU5402 for 1-hour periods starting from 9-13 hpf (a 10.5-11.5 hpf treatment is shown) produce subtler shape changes of the first pouch (arrowhead). (D,E) Flat-mount preparations of Alcian-stained pharyngeal cartilages at 4 days. In wild-type (D), mandibular M and PQ, hyoid CH and HS, and branchial CB1-5 cartilages are labeled. In those animals in which 10-14 hpf SU5402 treatment caused losses of the first pouch early, the HS cartilage was selectively absent later (E). Although M, PQ and CH cartilages are reduced in size, posterior CB cartilages are relatively unaffected. (F) Whereas later treatments with SU5402 (a 20-21 hpf treatment is shown) do not affect first pouch development (arrowhead), they do occasionally disrupt the formation of more posterior pouches (arrow shows an unsegmented branchial NCC mass). (G) Quantitation of first pouch defects after 4-hour treatments with SU5402. The percentages of animals with first pouch losses, in black, and misshapen first pouches, in gray, are plotted. $n_{6\text{-}10\ hpf}$=49, $n_{10\text{-}14\ hpf}$=99, $n_{14\text{-}18\ hpf}$=21. First pouch loss after 10-14 hpf treatment is statistically significant using Tukey HSD test. (H) The percentage of *fli1*-GFP animals having first pouch defects (primarily shape changes) plotted against the start time of 1 hour treatments with SU5402. $n_{5.5\ hpf}$=17, $n_{7\ hpf}$=14, $n_{8\ hpf}$=24, $n_{9\ hpf}$=14, $n_{10.5\ hpf}$=21, $n_{11\ hpf}$=18, $n_{12\ hpf}$=26, $n_{13\ hpf}$=26, $n_{14\ hpf}$=22, $n_{16\ hpf}$=26, $n_{20\ hpf}$=24, $n_{24\ hpf}$=31. The period of strongest effect is from 9 hpf (90% epiboly) to 13 hpf (8-somites). In order to assess the efficiency of inhibition of Fgf signaling, and the recovery after washout, we fixed sibling controls and examined *pea3* expression, a downstream effector of Fgf signaling, at 0 and 4 hours after washout. We know that SU5402 is at least partially being washed out as omission of the washout step leads to severe necrosis of animals. For 4-hour incubation experiments, the levels of *pea3* in individual animals, relative to those in similarly staged untreated controls, were as follows: 6-10 hpf, 6/8 reduced at 10 hpf, 11/13 reduced and 2/13 absent at 14 hpf; 10-14 hpf, 5/13 reduced and 8/13 absent at 14 hpf, 6/13 reduced and 7/13 absent at 18 hpf; 14-18 hpf, 5/12 reduced and 7/12 absent at 18 hpf. As *pea3* levels were similarly reduced at 18 hpf in 10-14 hpf and 14-18 hpf treatments, yet only 10-14 hpf treatments cause first pouch defects, we conclude that Fgf signaling is required from 10-14 hpf for first pouch development. However, these experiments do not exclude additional requirements for Fgf signaling at later times. Anterior is to the left and dorsal is up. M, Meckel's; PQ, palatoquadrate; CH, ceratohyal; HS, hyosymplectic; SU, SU5402. Scale bar: 50 μm.

shown). These results suggest that Fgf8 and Fgf3 act to promote the segmentation of pharyngeal endoderm into pouches and not endoderm generation.

Similarly, in order to understand the losses of the NCC-derived cartilages in *fgf8*$^{-}$; *fgf3*-MO animals, we examined the development of NCC in doubly reduced animals. In 18 hpf wild-type embryos, *dlx2* expression marked three postmigratory NCC masses: the mandibular, hyoid and branchial primordia (Fig. 6I). In *fgf3*-MO and *fgf8*$^{-}$ embryos, the three *dlx2*-positive masses resembled those in wild-type animals (Fig. 6J,K). By contrast, in *fgf8*$^{-}$; *fgf3*-MO embryos, only two *dlx2*-positive masses were present (Fig. 6L). Based

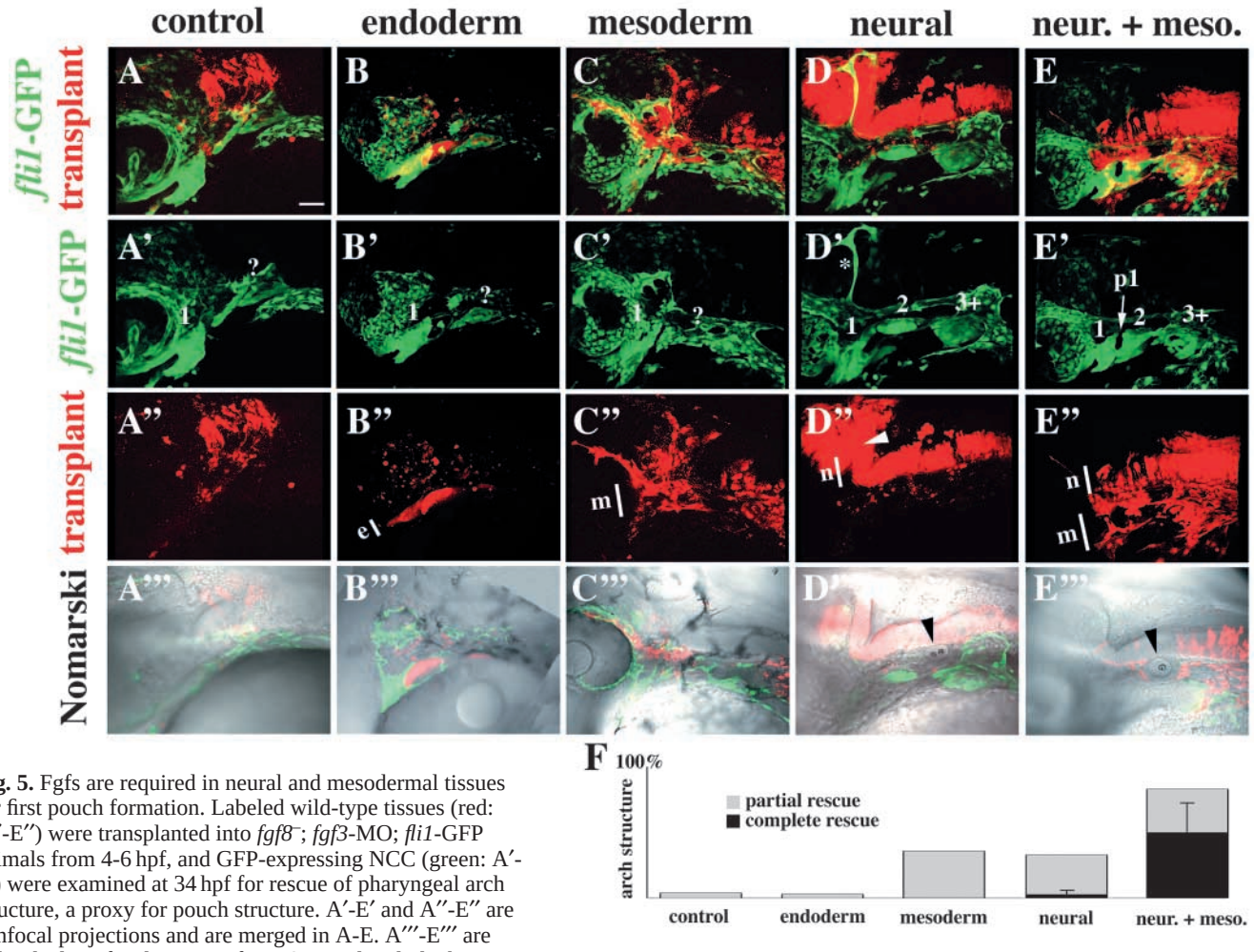

Fig. 5. Fgfs are required in neural and mesodermal tissues for first pouch formation. Labeled wild-type tissues (red: A″-E″) were transplanted into *fgf8*$^{-}$; *fgf3*-MO; *fli1*-GFP animals from 4-6 hpf, and GFP-expressing NCC (green: A′-E′) were examined at 34 hpf for rescue of pharyngeal arch structure, a proxy for pouch structure. A′-E′ and A″-E″ are confocal projections and are merged in A-E. A‴-E‴ are individual confocal sections from A-E and include the Nomarski channel. (A-A‴) As transplantations generally contribute donor tissue unilaterally, we used contralateral non-recipient sides of *fgf8*$^{-}$; *fgf3*-MO; *fli1*-GFP animals as negative controls for rescue (the red staining in A,A″ represents a comparatively small amount of donor tissue that has crossed the midline). In control sides, only mandibular (1) and a few unidentified (?) NCC are evident (A′), and the ear is missing (A‴). (B-B‴) Wild-type endoderm (e) fails to rescue pharyngeal arch structure (B′) and the ear (B‴). As seen in B″, wild-type endoderm does not segment into pouches in *fgf8*$^{-}$; *fgf3*-MO; *fli1*-GFP hosts. Wild-type mesoderm (m, C-C‴) or wild-type neural tissue (n, D-D‴) only partially rescues pharyngeal arch structure in a fraction of animals. In the non-rescued mesodermal example shown (C′), pharyngeal (1 + ?) NCC remain unsegmented, revealing a lack of pouches. The neural example shown (D′) represents what we scored as partial rescue of arch structure. There is an increase in the amount and organization of NCC, but they are not segmented into ordered pharyngeal arches as in wild-type animals. The lack of rescue of arch structure by wild-type neural tissue is striking, as other structures such as the MHB blood vessel (asterisk in D′), the neural flexure (white arrowhead in D″), and the ear (black arrowhead in D‴) are rescued by neural tissue. By contrast, wild-type mesoderm did not rescue the ear (C‴). (E-E‴) Both wild-type mesoderm and neural tissue are required together to completely rescue pharyngeal arch structure, and hence pouches, in *fgf8*$^{-}$; *fgf3*-MO; *fli1*-GFP animals. In this example, a morphologically normal first pouch (p1, arrow) and mandibular (1) and hyoid (2) arches are clearly seen (E′). Some of the more posterior pouches (E′, note the segmentation of the branchial (3+) NCC mass) and the ear (black arrowhead in E‴) are rescued as well. The identification of mesoderm in the transplants was based on the lack of colocalization with the neural crest marker *fli1*-GFP in confocal sections, and in this example by the characteristic morphology of the mesodermal cores of the pharyngeal arches (Kimmel et al., 2001) (F) Quantitation of pharyngeal arch rescue by wild-type tissues is plotted as percentage of host sides with complete (black) or partial (gray) rescue of arch structure. $n_{endoderm}$=34, $n_{mesoderm}$=11, n_{neural}=30, $n_{neural+mesoderm}$=6. Complete rescue by neural and mesodermal tissue (neur. + meso.) and partial rescue by mesoderm or neural tissue were statistically significant using Tukey HSD test. In addition, no rescue was seen by wild-type neural crest, a tissue that does not express either Fgf8 or Fgf3 (data not shown). Anterior is to the left and dorsal is up. Scale bar: 50 μm.

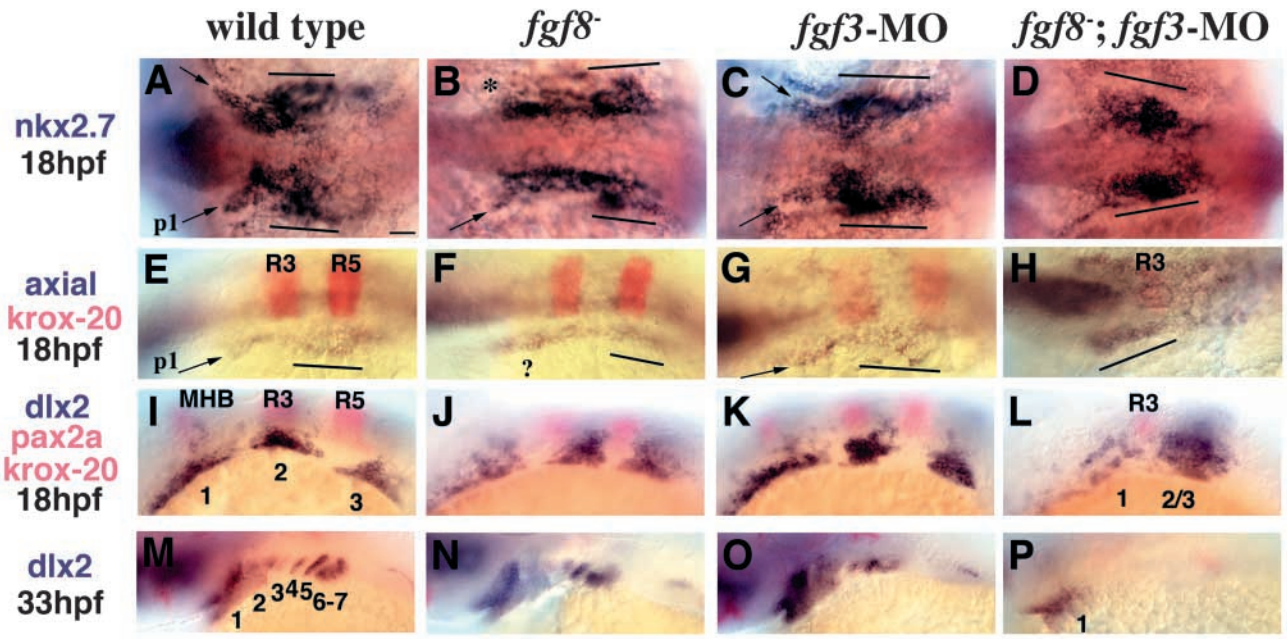

Fig. 6. Pharyngeal endoderm and cranial NCC defects in animals lacking Fgf8 and Fgf3. *nkx2.7* (A-D) and *axial* (E-H) label pharyngeal endoderm during early pouch morphogenesis stages (18 hpf). *nkx2.7* and *axial* are in blue, and, in E-H, *krox-20* in red labels R3 and R5. In wild-type animals (A,E), the first pouch (p1: arrows) has formed anterior to R3, and a more posterior endodermal mass that will give rise to the remaining pouches (black lines) is situated adjacent to R4-R6 territory. The first pouch is variably lost in *fgf8*$^{-}$ animals (asterisk in B, question mark in F). Whereas pharyngeal endoderm develops normally in *fgf3*-MO animals (C,G), in *fgf8*$^{-}$; *fgf3*-MO animals (D,H) pharyngeal endoderm is present as a single anterior mass (black line) and no pouches are evident. (I-P) *dlx2*, in blue, labels cranial NCC; in red (I-L), *pax2a* labels the MHB and *krox-20* labels R3 and R5. (I) In 18 hpf wild-type animals, mandibular (1), hyoid (2), and branchial (3) NCC streams give rise to seven pharyngeal arches. (M) At 33 hpf, the third branchial stream has generated arches 3-5 and arches 6 and 7 have yet to separate. In *fgf8*$^{-}$ (J,N) and *fgf3*-MO (K,O) animals, the migration and coalescence of NCC to form the pharyngeal arches is largely normal. In *fgf8*$^{-}$; *fgf3*-MO animals, the mandibular (1) stream is disorganized and hyoid and branchial streams are fused together (2/3) at 18 hpf (L). By 33 hpf (P), nearly all hyoid and branchial NCC are absent, and mandibular (1) NCC are present but reduced. Anterior is to the left in all panels. A-D are dorsal views, and E-P are lateral views. R3 and R5, rhombomeres 3 and 5; MHB, midbrain-hindbrain boundary; p1, first pouch. Scale bar: 50 μm.

on their positions with respect to the R3 domain of the hindbrain, we interpreted these two masses as a disorganized mandibular mass and a single fused mass incorporating hyoid and branchial NCC. As hyoid NCC are generated adjacent to R4 and branchial NCC develop adjacent to R6-R7 domains (Schilling and Kimmel, 1994; Trainor and Krumlauf, 2001), the NCC fusions are probably due to the absence of intervening R5-R6 territory in *fgf8*$^{-}$; *fgf3*-MO embryos (Maves et al., 2002; Walshe et al., 2002). We observed similar *dlx2* phenotypes at 12 hpf (data not shown). By 33 hpf, *dlx2* labeled the mandibular and hyoid arches and four branchial segments in wild-type animals (Fig. 6M). In *fgf3*-MO and *fgf8*$^{-}$ animals, *dlx2* expression was only mildly reduced compared with wild-type controls (Fig. 6N,O). However, *dlx2* expression in *fgf8*$^{-}$; *fgf3*-MO animals revealed that by 33 hpf most NCC were absent except for a reduced mandibular population (Fig. 6P). We observed similar NCC losses in *fgf8*$^{-}$; *fgf3*-MO animals based on the NCC expression of the *fli1*-GFP transgene (Fig. 1D). Moreover, the selective disappearance of hyoid and branchial NCC between 18 hpf and 33 hpf was consistent with the later specific losses of the hyoid and branchial cartilages in *fgf8*$^{-}$; *fgf3*-MO animals. In conclusion, we found requirements for Fgf8 and Fgf3 in both the early organization (12-18 hpf) and the later survival (33 hpf) of NCC.

Pharyngeal pouches form by the lateral migration of endodermal cells

Understanding the role of Fgfs in pouch formation requires a detailed knowledge of the cell behaviors underlying pouch development in wild-type animals. Surprisingly, little is known about the mechanism of pouch formation in any species. In order to investigate the morphogenesis of pouch endoderm directly, we made time-lapse recordings of Alexa568-labeled developing endoderm in H2A.F/Z:GFP; *fli1*-GFP zebrafish (10-30 hpf: see Movies 3, 4 in supplementary material). As labeled endoderm was generated by a combination of TAR* induction and transplantation techniques (see Materials and methods for details), a large fraction, but not all, of the endodermal cells can be seen in the recordings. H2A.F/Z:GFP labels the nucleus of every cell (Pauls et al., 2001) and helps to identify landmarks, whereas *fli1*-GFP labels postmigratory NCC. At 10 hpf of wild-type development, Alexa568-labeled pharyngeal endodermal cells were scattered along the surface of the yolk (Fig. 7A,A′), a distribution that closely resembled endodermal *axial* expression at this time (Reiter et al., 2001). Over the next 6 hours, endodermal cells underwent a medial migration and became increasingly packed together near the midline (Fig. 7B,B′ show a 14 hpf intermediate stage). Shortly after medial migration, endodermal cells that would give rise to the first pouch began to extend thin cytoplasmic processes

and migrate back out laterally (18 hpf: Fig. 7C,C′ and more clearly in Movie 4). At this time, the first postmigratory NCC began to turn on *fli1*-GFP. During the next few hours, endodermal cells continued to migrate laterally in a directed fashion, and by 22 hpf the first pouch was nearly fully formed (Fig. 7D,D′). In addition, clusters of endodermal cells situated periodically along the AP axis migrated laterally to form progressively more posterior pouches in an AP wave of development. By 30 hpf in this recording, the positions of the first three pouches were clearly seen relative to the *fli1*-GFP-labeled NCC of the arches (Fig. 7E,E′). In three wild-type recordings, the lateral migration of endodermal cells was observed to underlie the formation of all labeled pouches. We conclude that the directed lateral migration of periodically spaced endodermal cells is the mechanism that generates the pharyngeal pouches.

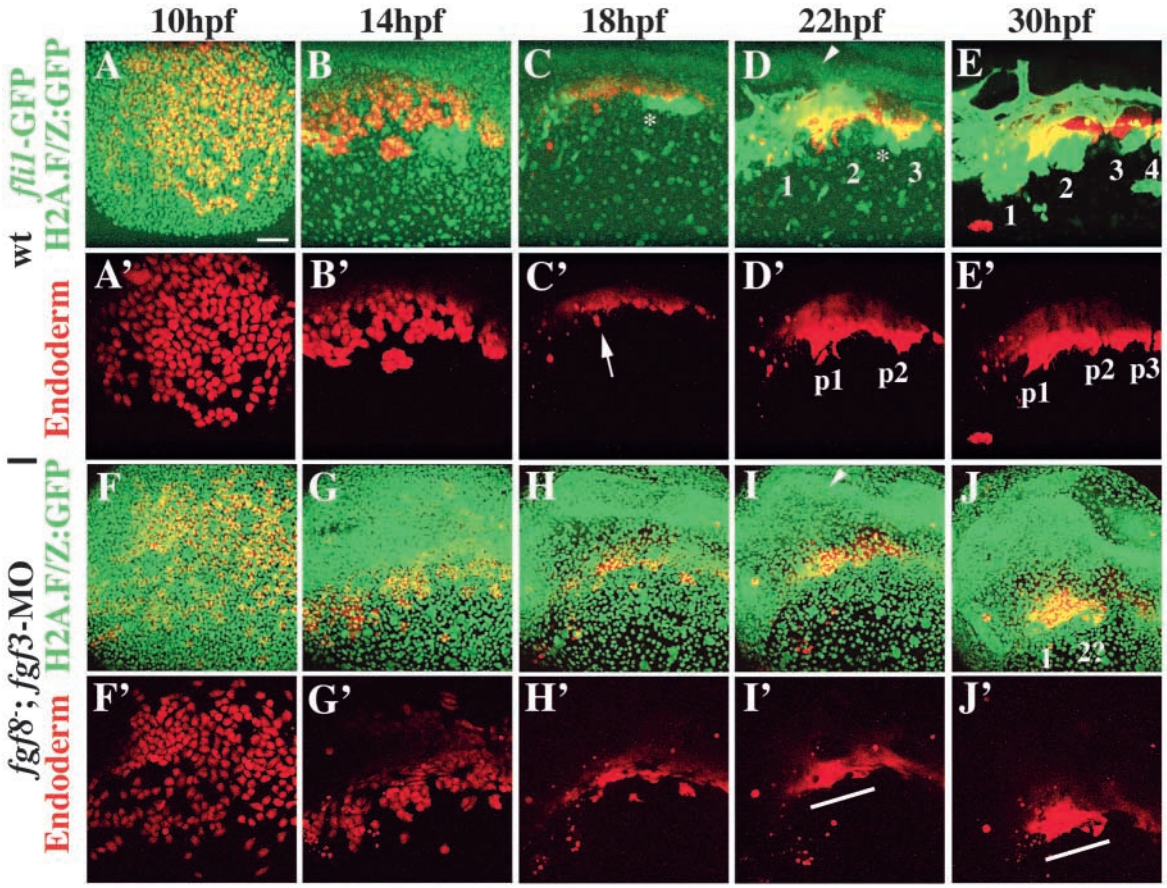

Fig. 7. Pharyngeal pouches form by an Fgf-dependent lateral migration of endodermal cells. (A-E) Representative still images from a time-lapse confocal recording of pharyngeal pouch and arch development in wild-type animals (see Movies 3, 4 in supplementary material). Pharyngeal endoderm has been labeled in red (A′-E′; merged with GFP in A-E) by transplanting TAR* endoderm into a *fli1*-GFP; H2A.F/Z:GFP host at 4 hpf; this technique leads to mosaic labeling of endoderm in the host animal. In green, H2A.F/Z:GFP allows the nuclei of every cell to be seen, and *fli1*-GFP marks NCC of the pharyngeal arches. In wild-type development, endodermal cells are spread out in a monolayer over the surface of the yolk at 10 hpf (A,A′). Concomitant with medial ectodermal movements to form the neural keel, endodermal cells migrate medially and begin to aggregate (14 hpf: B,B′). Shortly after medial migration, individual endodermal cells destined to become the first pouch (arrow in C′) then migrate back out laterally (C: 18 hpf). As seen in Movie 4, pouch endodermal cells extend cytoplasmic processes laterally during migration. At the same time, cranial NCC begin to condense and express *fli1*-GFP. By 22 hpf, the first two pouches (D′: p1,p2) have formed and interdigitate three NCC-containing pharyngeal arches (D: 1-3). Although in this example most second pouch cells are not labeled in red, their development can still be observed based on transient expression of *fli1*-GFP (asterisks in C,D). Also, the characteristic flexure of the neural keel near the MHB is visible by H2A.F/Z:GFP (arrowhead in D). At 30 hpf, three pouches (E′: p1-p3) and four arches (E: 1-4) are well developed. (F-J) Representative still images from a time-lapse recording of pharyngeal development in an animal reduced for Fgf8 and Fgf3 (see Movies 5, 6 in supplementary material). Similar cell behaviors were seen in two separate recordings. Labeled endoderm (red) was generated by transplantation of wild-type TAR* endoderm into *fgf8*$^{-}$; *fgf3*-MO; H2A.F/Z:GFP animals (see text for discussion of experimental rationale, including how wild-type and mutant endoderm probably behave similarly in a mutant host). In *fgf8*$^{-}$; *fgf3*-MO animals, the generation (F,F′) and medial migration (G,G′) of pharyngeal endoderm is normal. However, by 18 hpf, the lateral migration of endodermal cells is delayed (H,H′). Also, the migration of endodermal cells is disorganized, with cytoplasmic processes not being oriented laterally as in wild-type animals (arrows in Movie 6 in supplementary material). By 22 hpf lateral endodermal cells form an extended anterior mass (white line in I′). A confirmation of the *fgf8*$^{-}$; *fgf3*-MO phenotype is the lack of a neural flexure (arrowhead in I), increased cell death at the MHB, and the lack of an ear (data not shown). By 30 hpf, pharyngeal endoderm has not segmented into discrete pouches and remains a single anterior mass (white line in J′). Although animals did not carry the *fli1*-GFP transgene, reduced mandibular (1) and possibly hyoid (2?) arches are visible as condensations of H2A.F/Z:GFP-expressing cells. The views are dorsolateral with anterior to the left. Scale bar: 50 μm.

Fgfs are required for the segmentation and directed migration of endodermal cells that form pouches

In order to understand the cellular basis for the lack of pouches in animals reduced for Fgf8 and Fgf3, we made time-lapse recordings of pharyngeal endoderm development in *fgf8*$^{-}$; *fgf3*-MO; H2A.F/Z:GFP animals (10-30 hpf: see Movies 5, 6 in supplementary material). For technical reasons, we visualized pharyngeal endoderm by transplanting labeled, TAR*-induced endoderm from wild-type donors into *fgf8*$^{-}$; *fgf3*-MO; H2A.F/Z:GFP hosts (see Materials and methods). However, as we knew that wild-type endoderm failed to make pouches in an *fgf8*$^{-}$; *fgf3*-MO background, we inferred that the endoderm defects we describe here would be the same as in non-mosaic *fgf8*$^{-}$; *fgf3*-MO animals. At 10 hpf, we saw a similar distribution of pharyngeal endodermal cells over the surface of the yolk as in wild-type animals (Fig. 7F,F′), consistent with our earlier finding that *fgf8*$^{-}$; *fgf3*-MO animals had no defect in 10 hpf endodermal *axial* expression. In addition, the medial migration and subsequent compaction of endodermal cells near the midline was largely normal in *fgf8*$^{-}$; *fgf3*-MO animals (Fig. 7G-H′). However, by 18 hpf we saw defects in the lateral migration of endodermal cells (Fig. 7H,H′). Although endodermal cells extended cytoplasmic processes in *fgf8*$^{-}$; *fgf3*-MO animals, these processes were not always directed laterally and often retracted (see Movie 6 in supplementary material). By 22 hpf, endodermal cells had failed to migrate laterally and discrete pouches were not seen (Fig. 7I,I′). Moreover, putative pouch endodermal cells did not align into regularly spaced arrays and by 30 hpf had formed a single, unsegmented clump of cells laterally (Fig. 7J,J′). We conclude that Fgf8 and Fgf3 are not required for the initial generation or medial migration of pharyngeal endodermal cells. Instead, Fgfs have later functions in the directed lateral migration and regular spacing of pharyngeal endodermal cells along the AP axis, processes critical for the formation of discrete pouches.

Discussion

Pharyngeal pouches form by an Fgf-dependent lateral migration of endodermal cells

We have demonstrated an essential role for Fgf signaling in the formation of pharyngeal pouches. Whereas *fgf8*$^{-}$ animals had variable defects in pouch formation, animals reduced for both Fgf8 and Fgf3 lacked all pharyngeal pouches. In addition, transient inhibition of Fgf signaling with the Fgf receptor antagonist SU5402 caused similar defects in pouch formation. This essential function of Fgfs in pouch formation is probably conserved among vertebrates, as mice hypomorphic for *Fgf8* or *Fgf receptor 1* (*FgfR1*) have similar pouch defects to those in *fgf8*$^{-}$ zebrafish (Abu-Issa et al., 2002; Trokovic et al., 2003).

Previous to this study, little was known about the cellular behaviors underlying pouch formation. Pharyngeal pouches arise as lateral branches of the foregut endoderm. Branching morphogenesis is a common theme in organogenesis, and various cellular mechanisms, such as clefting and cell migration, have been implicated in branch generation (Chuang and McMahon, 2003; Ghabrial et al., 2003; Sakai et al., 2003). By directly imaging pouch formation in developing zebrafish embryos, we showed that cell migration is the mechanism that drives the lateral branching of the pharyngeal endoderm into pouches. After coalescence of pharyngeal endoderm near the ventral midline, subsets of endodermal cells migrated laterally at periodic intervals along the AP axis to form pouches. As cells could be seen extending cytoplasmic processes laterally during migration, we propose that chemotactic or substrate cues in the local environment guide pouch endodermal cells to lateral positions.

Several lines of evidence indicate that the lack of pouches in *fgf8*$^{-}$; *fgf3*-MO animals is probably due to a defect in the later morphogenesis of pouch endoderm. Based on the expression of endodermal markers such as *axial* and *nkx2.7*, pharyngeal endoderm was present in *fgf8*$^{-}$; *fgf3*-MO animals, although we do not know if mediolateral patterning of the endoderm was completely normal. Whereas *axial* and *nkx2.7* expression suggest that pouch formation was defective at early stages in *fgf8*$^{-}$; *fgf3*-MO animals, a lack of pouch formation was clearly seen later using the Zn8 antibody or transplant techniques to label endoderm. A role for Fgfs in the morphogenesis of pouch endoderm was most evident in time-lapse recordings of endodermal development in *fgf8*$^{-}$; *fgf3*-MO embryos. Whereas the generation, medial migration and coalescence of endodermal cells were largely normal, we saw defects in both the later lateral migration and AP positioning of pharyngeal endodermal cells in *fgf8*$^{-}$; *fgf3*-MO embryos. The migration of endodermal cells was delayed, and the thin cytoplasmic processes characteristic of migrating cells were disorganized in *fgf8*$^{-}$; *fgf3*-MO embryos. Thus, in the absence of Fgfs, putative pouch endodermal cells had the ability to migrate but could not orient themselves along the mediolateral axis. In addition, whereas in wild-type embryos pouch endodermal cells migrated laterally at periodic AP positions, in *fgf8*$^{-}$; *fgf3*-MO embryos endodermal cells remained a continuous mass occupying the anterior pharyngeal region. We propose that Fgf signaling may regulate both the migration and AP positioning of pouch endodermal cells, and future experiments are needed to elucidate the extent to which these processes are interrelated.

How do neural and mesodermal Fgfs pattern pharyngeal pouches?

Our transplantation experiments demonstrated that Fgf8 and Fgf3 are required additively in the neural keel and head mesoderm to rescue first pouch formation in *fgf8*$^{-}$; *fgf3*-MO embryos. Consistent with this, inhibition of Fgf signaling from tailbud (10 hpf) to 10-somites (14 hpf), stages at which Fgf8 and Fgf3 are expressed in the neural keel and lateral mesoderm, blocked first pouch formation. An attractive model is that signals from the neural keel help to pattern both the pharyngeal endoderm and premigratory NCC (Fig. 8A). Such a strategy would link the two sources of pharyngeal segmentation, segmentation of NCC into distinct streams and segmentation of the endoderm into pouches, to the earlier segmentation of the hindbrain. Intriguingly, mandibular NCC originate from ectomesenchyme adjacent to the MHB and are Hox-negative, and the first pharyngeal pouch develops in the vicinity of MHB-R2 and is also Hox-negative (Hunt et al., 1991; Miller et al., 2004). By contrast, the second pouch and hyoid NCC develop adjacent to R4 and are both Hox-positive. Whereas development of the first two pouches connects to segmental expression of Fgf in the hindbrain, it is less clear how development of the more posterior pouches would be regulated. All pouches were lost in animals lacking both Fgf8

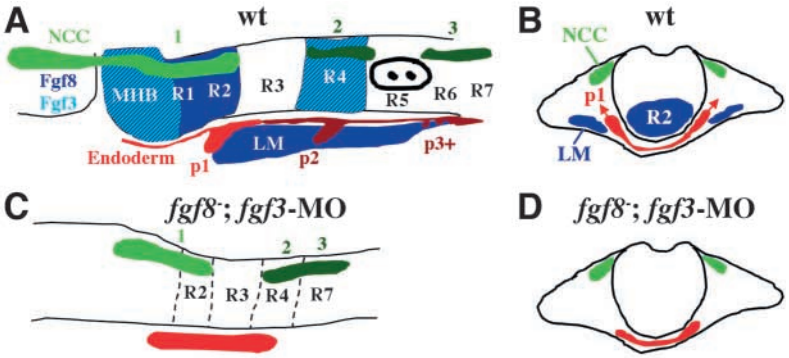

Fig. 8. Fgf8 and Fgf3 as positional determinants of pharyngeal segmentation. Model of pharyngeal segmentation in wild type (A,B) and animals lacking Fgf8 and Fgf3 (C,D). This model is based on *fgf8* expression (Reifers et al., 2000) and *fgf3* expression (Maves et al., 2002) at 13 hpf (8-somites). A and C are lateral views with anterior to the left and dorsal up, and B and D are cross-sectional views at the level of R2. (A,B) In wild type, Fgf8 protein, dark blue, is produced in neural MHB-R2 and R4 domains and in the lateral mesoderm. Fgf3 protein, light blue, is co-produced with Fgf8 in the MHB and R4 (striped domains represent overlap). Mandibular (1) NCC (Hox negative: light green) are generated adjacent to MHB-R2 territory, whereas hyoid (2) and branchial (3) NCC (Hox positive: dark green) have their origins at R4 and R6-R7 axial levels, respectively. Likewise, the first (p1) endodermal pouch (Hox negative: red) develops ventrolateral to R2, and the second (p2) and more posterior (p3+) pouches (Hox positive: wine) form ventrolateral to R4 and R6-R7, respectively. The ear (black circle with two dots) develops adjacent to R5. (B) A cross-sectional view shows that during lateral migration pouch endodermal cells are in close proximity to Fgf-expressing ventral neural keel and lateral mesoderm. Pharyngeal pouches would form where Fgf expression in the hindbrain coincides with Fgf8 expression in the underlying lateral mesoderm. (C,D) In *fgf8*$^{-}$; *fgf3*-MO animals, NCC and pharyngeal endoderm are generated but subsequent morphogenesis is defective. Pharyngeal endoderm remains unsegmented and hyoid and branchial NCC streams fuse. The structure of the hindbrain is also defective in animals lacking Fgf8 and Fgf3. MHB, R1, R5 and R6 regions fail to develop, and R2 and R3 are reduced in size (Brand et al., 1996; Walshe et al., 2002; Maves et al., 2002; Reifers et al., 1998). As Fgfs are required in both neural and mesodermal tissues to promote the formation of pouches, Fgf signaling may link early neural and mesodermal patterning to segmentation of the pharyngeal endoderm. In a direct model, Fgfs from the lateral mesoderm and ventral hindbrain act as chemoattractants to promote the lateral migration of pouch endodermal cells (B). In animals lacking Fgf8 and Fgf3, pouch endodermal cells would fail to get the appropriate cues to migrate laterally (D). Alternatively, in an indirect model, Fgfs function to regulate the structure of, and gene expression in, the hindbrain and lateral mesoderm. In the absence of Fgf signaling, guidance cues for pouch endodermal migration would be reduced or absent. LM, lateral mesoderm; MHB, midbrain–hindbrain boundary; R, rhombomere.

and Fgf3, and transient inhibition of Fgf signaling, at times later than those used to inhibit first pouch formation, disrupted the formation of more posterior pouches. However, pouches three through six develop at stages when Fgfs are no longer expressed in the hindbrain and head mesoderm. Further analysis will be required to determine how similar the functions of Fgfs in posterior pouch formation are to those described here for first pouch formation.

Although we showed that Fgfs are essential for pouch morphogenesis, our results do not distinguish between direct and indirect functions of Fgfs in pouch outgrowth. For example, Fgfs from the lateral mesoderm may act directly as chemoattractants for the lateral migration of pharyngeal endodermal cells. In *Drosophila*, the branching of the trachea also requires Fgf signaling (Klambt et al., 1992; Sutherland et al., 1996), and tracheal cells have been shown to migrate toward ectopic sources of Fgf (Sato and Kornberg, 2002). Alternatively, Fgfs may influence pouch formation indirectly by regulating patterning of the hindbrain and lateral mesoderm. By 16 hpf, pharyngeal endodermal cells in close proximity ventrally to the neural keel and medially to lateral mesoderm begin to migrate to form the pouches (Fig. 8B). However, we could block first pouch formation by inhibiting Fgf signaling from 10-14 hpf, although we cannot rule out that there is a delay between addition of the drug and effective inhibition of Fgf signaling. In one model, the role of Fgfs would be to establish segmental signals in the hindbrain that control the later lateral migration of endodermal cells at periodic positions along the AP axis. Consistent with this, animals reduced for Fgf8 and Fgf3 have hindbrain defects that include losses of MHB and segments R1, R5 and R6, and reductions in size of additional rhombomeres (Walshe et al., 2002; Maves et al., 2002). If pouch endodermal cells are responding to segmental cues in the hindbrain for their migration, the reduced size and segmentation of the hindbrain may explain why endodermal cells did not migrate at discrete AP positions and ultimately formed compressed clumps in *fgf8*$^{-}$; *fgf3*-MO animals (Fig. 8C,D). In addition, as *fgf8*$^{-}$ but not *fgf3*-MO zebrafish have defects in MHB structure (Reifers et al., 1998), a lack of early Fgf8-dependent MHB signals might explain why *fgf8*$^{-}$ but not *fgf3*-MO embryos had variable first pouch defects. Similarly, Fgf8 has been shown to control both the gene expression profile and morphogenesis of the lateral head mesoderm (Reifers et al., 2000). Thus, Fgfs might promote pouch formation indirectly by controlling the positioning and expression of pouch guidance factors in the hindbrain and lateral mesoderm. Future experiments that address where Fgf signaling is required, for example by manipulating Fgf receptor function in the endoderm and other tissues, should help to clarify how directly Fgfs act to control pouch formation.

Pharyngeal pouches pattern cartilages of the hyoid and branchial arches

In *fgf8*$^{-}$; *fgf3*-MO animals, no pouches formed and little or no cartilage was made from the Hox-expressing NCC of the hyoid and branchial arches. Similarly, transient inhibition of Fgf signaling during early somite stages led to correlated losses of both the first pouch and dorsal hyoid cartilage. However, in *fgf8*$^{-}$; *fgf3*-MO animals, mandibular cartilages, which are derived from NCC that do not express Hox genes, were less affected. By contrast, *cas* mutant zebrafish lack all endoderm and are missing cartilages derived from all pharyngeal arches (David et al., 2002), implying that Fgf-independent endodermal signals pattern cartilages of the mandibular arch. As pharyngeal endoderm was present but not segmented into pouches in *fgf8*$^{-}$; *fgf3*-MO animals, we conclude that the

outpocketing of the pharyngeal endoderm to form pouches is a critical event that allows endoderm to induce cartilage in Hox-positive NCC.

By analyzing individual sides of *fgf8*– animals, we found a correlation between early changes in pouch structure and later rearrangements of the cartilage pattern. In our studies of *integrinα5* mutant zebrafish, we found that the first pouch promotes the local compaction and survival of NCC that give rise to specific regions of dorsal hyoid cartilage (Crump et al., 2004). In *fgf8* mutant sides in which the first pouch was shifted in position or an ectopic pouch formed in presumptive hyoid NCC territory, we observed similar positional shifts of dorsal hyoid cartilage or ectopic cartilage elements. These correlations are consistent with the abnormal first pouch promoting hyoid cartilage development in abnormal locations. In other cases a deformed first pouch invaded NCC territory that, based on our previous fate mapping (Crump et al., 2004), normally forms dorsal hyoid cartilage, and this deformed pouch was correlated with a subsequent loss of dorsal hyoid cartilage. In addition, defects in the formation of more posterior pouches were correlated with losses and fusions of the ceratobranchial cartilages. Thus, whereas early pouch defects are largely predictive of later cartilage alterations, the precise interpretation of the resultant cartilage defects in *fgf8*– animals is complicated by the fact that Fgf8 probably has multiple functions in pharyngeal cartilage development.

Our finding that pharyngeal pouches were essential sources of patterning information for the cartilages of the Hox-expressing hyoid and branchial arches is consistent with work in chicken showing that different types of foregut endoderm interact with Hox-expressing versus non-Hox-expressing NCC to specify cartilage pattern. In these studies, involving the transplantation and ablation of endoderm domains at stages prior to pouch morphogenesis, anterior endoderm can respecify cartilage pattern when transplanted adjacent to Hox-negative, but not Hox-positive, NCC (Couly et al., 2002). However, more posterior endoderm can respecify cartilages derived from Hox-positive NCC (Ruhin et al., 2003). Based on our analysis of Fgf function in zebrafish, we predict that the posterior endoderm domains that induce cartilage from Hox-positive NCC in chicken will include endodermal regions that form pharyngeal pouches during later embryogenesis.

Lastly, what are the pouch-derived factors that promote cartilage development? Recent evidence suggests that Fgfs themselves are expressed later in the pouches and promote the survival of skeletogenic NCC. Studies in zebrafish have shown that Fgf3 is required in the pharyngeal endoderm for the survival of hyoid and branchial NCC (David et al., 2002; Nissen et al., 2003). As Fgf8 is also expressed, albeit less strongly, in the pouches, it has been proposed that Fgf8 may act redundantly with Fgf3 as an endoderm-derived NCC survival factor (Walshe and Mason, 2003a). Interestingly, we did observe graded reductions of dorsal hyoid cartilage in some *fgf8*– animals that had normal first pouches, consistent with Fgf8 also having a role in the later survival of NCC. Moreover, the lack of hyoid and branchial cartilages in *fgf8*–; *fgf3*-MO animals is most consistent with a survival defect of postmigratory Hox-positive NCC. Based on *dlx2* expression, hyoid and branchial NCC are present early but disappear later in *fgf8*–; *fgf3*-MO animals. However, as pouches do not form in *fgf8*–; *fgf3*-MO animals, the NCC survival defects are probably due in part to there being no pouches to secrete survival factors such as Fgf8 and Fgf3. As has been observed in tooth and lung development (Chuang and McMahon, 2003; Jernvall and Thesleff, 2000), it is becoming apparent that Fgfs also have multiple, temporally distinct functions during pharyngeal ontogeny. We propose that, in addition to a later function as pouch-derived survival factors, an essential early function of Fgfs in endodermal pouch morphogenesis may help explain the diversity of craniofacial phenotypes seen in *fgf8*– animals.

We thank John Dowd and the UO Fish Facility for abundant help with raising fish; Jose Campos-Ortega for providing the H2A.F/Z:GFP line before publication; Craig T. Miller, Le Trinh, Nick Osborne and Tom Schilling for helpful discussions, especially about endoderm; and Johann Eberhart for comments on the manuscript. J.G.C. is an O'Donnell Fellow of the Life Sciences Research Foundation. L.M. was supported by a fellowship from the Damon Runyon-Walter Winchell Cancer Research Fund. Research is funded by NIH grants DE13834 and HD22486.

Supplementary material

Supplementary material for this article is available at
http://dev.biologists.org/cgi/content/full/131/22/5703/DC1

References

Abu-Issa, R., Smyth, G., Smoak, I., Yamamura, K. and Meyers, E. N. (2002). Fgf8 is required for pharyngeal arch and cardiovascular development in the mouse. *Development* **129**, 4613-4625.

Akimenko, M. A., Ekker, M., Wegner, J., Lin, W. and Westerfield, M. (1994). Combinatorial expression of three zebrafish genes related to distal-less: part of a homeobox gene code for the head. *J. Neurosci.* **14**, 3475-3486.

Alexander, J., Rothenberg, M., Henry, G. L. and Stainier, D. Y. (1999). casanova plays an early and essential role in endoderm formation in zebrafish. *Dev. Biol.* **215**, 343-357.

Brand, M., Heisenberg, C. P., Jiang, Y. J., Beuchle, D., Lun, K., Furutani-Seiki, M., Granato, M., Haffter, P., Hammerschmidt, M., Kane, D. A. et al. (1996). Mutations in zebrafish genes affecting the formation of the boundary between midbrain and hindbrain. *Development* **123**, 179-190.

Brown, L. A., Amores, A., Schilling, T. F., Jowett, T., Baert, J. L., de Launoit, Y. and Sharrocks, A. D. (1998). Molecular characterization of the zebrafish PEA3 ETS-domain transcription factor. *Oncogene* **17**, 93-104.

Chuang, P. T. and McMahon, A. P. (2003). Branching morphogenesis of the lung: new molecular insights into an old problem. *Trends Cell Biol.* **13**, 86-91.

Couly, G., Creuzet, S., Bennaceur, S., Vincent, C. and le Douarin, N. M. (2002). Interactions between Hox-negative cephalic neural crest cells and the foregut endoderm in patterning the facial skeleton in the vertebrate head. *Development* **129**, 1061-1073.

Crump, J. G., Swartz, M. E. and Kimmel, C. B. (2004). An integrin-dependent role of pouch endoderm in hyoid cartilage development. *PLoS Biol.* **2**, E244.

David, N. B., Saint-Etienne, L., Tsang, M., Schilling, T. F. and Rosa, F. M. (2002). Requirement for endoderm and FGF3 in ventral head skeleton formation. *Development* **129**, 4457-4468.

Draper, B. W., Morcos, P. A. and Kimmel, C. B. (2001). Inhibition of zebrafish fgf8 pre-mRNA splicing with morpholino oligos: a quantifiable method for gene knockdown. *Genesis* **30**, 154-156.

Fashena, D. and Westerfield, M. (1999). Secondary motoneuron axons localize DM-GRASP on their fasciculated segments. *J. Comp. Neurol.* **406**, 415-424.

Ghabrial, A., Luschnig, S., Metzstein, M. M. and Krasnow, M. A. (2003). Branching morphogenesis of the Drosophila tracheal system. *Annu. Rev. Cell Dev. Biol.* **19**, 623-647.

Hauptmann, G. and Gerster, T. (1994). Two-color whole-mount in situ hybridization to vertebrate and Drosophila embryos. *Trends Genet.* **10**, 266.

Hunt, P., Gulisano, M., Cook, M., Sham, M. H., Faiella, A., Wilkinson, D., Boncinelli, E. and Krumlauf, R. (1991). A distinct Hox code for the branchial region of the vertebrate head. *Nature* **353**, 861-864.

Jernvall, J. and Thesleff, I. (2000). Reiterative signaling and patterning during mammalian tooth morphogenesis. *Mech. Dev.* **92**, 19-29.

Jowett, T. and Lettice, L. (1994). Whole-mount in situ hybridizations on zebrafish embryos using a mixture of digoxigenin- and fluorescein-labelled probes. *Trends Genet.* **10**, 73-74.

Kimmel, C. B., Warga, R. M. and Schilling, T. F. (1990). Origin and organization of the zebrafish fate map. *Development* **108**, 581-594.

Kimmel, C. B., Ballard, W. W., Kimmel, S. R., Ullmann, B. and Schilling, T. F. (1995). Stages of embryonic development of the zebrafish. *Dev. Dyn.* **203**, 253-310.

Kimmel, C. B., Miller, C. T. and Moens, C. B. (2001). Specification and morphogenesis of the zebrafish larval head skeleton. *Dev. Biol.* **233**, 239-257.

Klambt, C., Glazer, L. and Shilo, B. Z. (1992). breathless, a Drosophila FGF receptor homolog, is essential for migration of tracheal and specific midline glial cells. *Genes Dev.* **6**, 1668-1678.

Kontges, G. and Lumsden, A. (1996). Rhombencephalic neural crest segmentation is preserved throughout craniofacial ontogeny. *Development* **122**, 3229-3242.

Krauss, S., Johansen, T., Korzh, V. and Fjose, A. (1991). Expression of the zebrafish paired box gene pax[zf-b] during early neurogenesis. *Development* **113**, 1193-1206.

Lawson, N. D. and Weinstein, B. M. (2002). In vivo imaging of embryonic vascular development using transgenic zebrafish. *Dev. Biol.* **248**, 307-318.

Le Douarin, N. M. (1982). *The neural crest*. Cambridge, UK: Cambridge University Press.

Lee, K. H., Xu, Q. and Breitbart, R. E. (1996). A new tinman-related gene, nkx2.7, anticipates the expression of nkx2.5 and nkx2.3 in zebrafish heart and pharyngeal endoderm. *Dev. Biol.* **180**, 722-731.

Maroon, H., Walshe, J., Mahmood, R., Kiefer, P., Dickson, C. and Mason, I. (2002). Fgf3 and Fgf8 are required together for formation of the otic placode and vesicle. *Development* **129**, 2099-2108.

Maves, L., Jackman, W. and Kimmel, C. B. (2002). FGF3 and FGF8 mediate a rhombomere 4 signaling activity in the zebrafish hindbrain. *Development* **129**, 3825-3837.

Miller, C. T., Yelon, D., Stainier, D. Y. and Kimmel, C. B. (2003). Two endothelin 1 effectors, hand2 and bapx1, pattern ventral pharyngeal cartilage and the jaw joint. *Development* **130**, 1353-1365.

Miller, C. T., Maves, L. and Kimmel, C. B. (2004). moz regulates Hox expression and pharyngeal segmental identity in zebrafish. *Development* **131**, 2443-2461.

Nissen, R. M., Yan, J., Amsterdam, A., Hopkins, N. and Burgess, S. M. (2003). Zebrafish foxi one modulates cellular responses to Fgf signaling required for the integrity of ear and jaw patterning. *Development* **130**, 2543-2554.

Odenthal, J. and Nusslein-Volhard, C. (1998). fork head domain genes in zebrafish. *Dev. Genes Evol.* **208**, 245-258.

Oxtoby, E. and Jowett, T. (1993). Cloning of the zebrafish krox-20 gene (krx-20) and its expression during hindbrain development. *Nucleic Acids Res.* **21**, 1087-1095.

Pauls, S., Geldmacher-Voss, B. and Campos-Ortega, J. A. (2001). A zebrafish histone variant H2A.F/Z and a transgenic H2A.F/Z:GFP fusion protein for in vivo studies of embryonic development. *Dev. Genes Evol.* **211**, 603-610.

Phillips, B. T., Bolding, K. and Riley, B. B. (2001). Zebrafish fgf3 and fgf8 encode redundant functions required for otic placode induction. *Dev. Biol.* **235**, 351-365.

Piotrowski, T. and Nusslein-Volhard, C. (2000). The endoderm plays an important role in patterning the segmented pharyngeal region in zebrafish (Danio rerio). *Dev. Biol.* **225**, 339-356.

Reifers, F., Bohli, H., Walsh, E. C., Crossley, P. H., Stainier, D. Y. and Brand, M. (1998). Fgf8 is mutated in zebrafish acerebellar (ace) mutants and is required for maintenance of midbrain-hindbrain boundary development and somitogenesis. *Development* **125**, 2381-2395.

Reifers, F., Walsh, E. C., Leger, S., Stainier, D. Y. and Brand, M. (2000). Induction and differentiation of the zebrafish heart requires fibroblast growth factor 8 (fgf8/acerebellar). *Development* **127**, 225-235.

Reiter, J. F., Kikuchi, Y. and Stainier, D. Y. (2001). Multiple roles for Gata5 in zebrafish endoderm formation. *Development* **128**, 125-135.

Roehl, H. and Nusslein-Volhard, C. (2001). Zebrafish pea3 and erm are general targets of FGF8 signaling. *Curr. Biol.* **11**, 503-507.

Ruhin, B., Creuzet, S., Vincent, C., Benouaiche, L., le Douarin, N. M. and Couly, G. (2003). Patterning of the hyoid cartilage depends upon signals arising from the ventral foregut endoderm. *Dev. Dyn.* **228**, 239-246.

Sakai, T., Larsen, M. and Yamada, K. M. (2003). Fibronectin requirement in branching morphogenesis. *Nature* **423**, 876-881.

Sato, M. and Kornberg, T. B. (2002). FGF is an essential mitogen and chemoattractant for the air sacs of the drosophila tracheal system. *Dev. Cell* **3**, 195-207.

Schilling, T. F. and Kimmel, C. B. (1994). Segment and cell type lineage restrictions during pharyngeal arch development in the zebrafish embryo. *Development* **120**, 483-494.

Sutherland, D., Samakovlis, C. and Krasnow, M. A. (1996). branchless encodes a Drosophila FGF homolog that controls tracheal cell migration and the pattern of branching. *Cell* **87**, 1091-1101.

Trainor, P. A. and Krumlauf, R. (2001). Hox genes, neural crest cells and branchial arch patterning. *Curr. Opin. Cell Biol.* **13**, 698-705.

Trevarrow, B., Marks, D. L. and Kimmel, C. B. (1990). Organization of hindbrain segments in the zebrafish embryo. *Neuron* **4**, 669-679.

Trokovic, N., Trokovic, R., Mai, P. and Partanen, J. (2003). Fgfr1 regulates patterning of the pharyngeal region. *Genes Dev.* **17**, 141-153.

Tucker, A. S., Yamada, G., Grigoriou, M., Pachnis, V. and Sharpe, P. T. (1999). Fgf-8 determines rostral-caudal polarity in the first branchial arch. *Development* **126**, 51-61.

Walshe, J. and Mason, I. (2003a). Fgf signalling is required for formation of cartilage in the head. *Dev. Biol.* **264**, 522-536.

Walshe, J. and Mason, I. (2003b). Unique and combinatorial functions of Fgf3 and Fgf8 during zebrafish forebrain development. *Development* **130**, 4337-4349.

Walshe, J., Maroon, H., McGonnell, I. M., Dickson, C. and Mason, I. (2002). Establishment of hindbrain segmental identity requires signaling by FGF3 and FGF8. *Curr. Biol.* **12**, 1117-1123.

Westerfield, M. (1995). *The Zebrafish Book*. Eugene, OR: University of Oregon.

Weston, J. A., Yoshida, H., Robinson, V., Nishikawa, S. and Fraser, S. T. (2004). Neural crest and the origin of ectomesenchyme: neural fold heterogeneity suggests an alternative hypothesis. *Dev. Dyn.* **229**, 118-130.

Wilson, J. and Tucker, A. S. (2004). Fgf and Bmp signals repress the expression of Bapx1 in the mandibular mesenchyme and control the position of the developing jaw joint. *Dev. Biol.* **266**, 138-150.